

Enhanced Cooper Pairing via Random Matrix Phonons in Superconducting Grains

Andrey Grankin,¹ Mohammad Hafezi,¹ and Victor Galitski¹

¹*Joint Quantum Institute, Department of Physics,
University of Maryland, College Park, MD 20742, USA*

There is rich experimental evidence that granular superconductors and superconducting films often exhibit a higher transition temperature, T_c , than that in bulk samples of the same material. This paper suggests that this enhancement hinges on random matrix phonons mediating Cooper pairing more efficiently than bulk phonons. We develop the Eliashberg theory of superconductivity in chaotic grains, calculate the random phonon spectrum and solve the Eliashberg equations numerically. Self-averaging of the effective electron-phonon coupling constant is noted, which allows us to fit the numerical data with analytical results based on a generalization of the Berry conjecture. The key insight is that the phonon density of states, and hence T_c , shows an enhancement proportional to the ratio of the perimeter and area of the grain - the Weyl law. We benchmark our results for aluminum films, and find an enhancement of T_c of about 10% for a randomly-generated shape. A larger enhancement of T_c is readily possible by optimizing grain geometries. We conclude by noticing that mesoscopic shape fluctuations in realistic granular structures should give rise to a further enhancement of global T_c due to the formation of a percolating Josephson network.

The Bardeen-Cooper-Schrieffer (BCS) theory of superconductivity is a rare example of a controlled theory with a quantitative relevance to experiment. It has been tremendously successful not only in explaining the origin of superconductivity, but also in accurately estimating the transition temperature in a variety of conventional phonon-driven superconductors. However, despite this success, there exists an extensive range of experimental phenomenology on granular superconductors, disordered films, and layered structures dating from the 1940s up to these days that remains largely unexplained [1-6]. Paradoxically, it has been observed that making superconducting structures more random and granular often leads to an increase of the superconducting transition temperature, T_c , sometimes exhibiting many-fold increase [1] of T_c compared to bulk three-dimensional samples. Unfortunately, the standard computational material science techniques are not informative in this context, because the underlying band theory breaks down.

This work develops the theory of superconducting pairing in mesoscopic grains. A generic grain boundary defines a chaotic billiard, and therefore both the electron [7, 8] and phonon spectra follow random matrix theory [9]. These spectra are eigenvalues of the elliptic differential operators originating - the single-particle Schrödinger equation for electrons and the wave equation for phonons. In the simplest case of an elementary metal (e.g., aluminum) only acoustic modes are relevant [10]. The Debye model further reduces the problem to solving the Laplace equation for transverse and longitudinal phonons, which are coupled through non-trivial boundary conditions, $n_i \sigma_{ij} \Big|_{\text{boundary}} = 0$ [9, 11, 12], where \mathbf{n} is normal to the boundary and $\hat{\sigma}$ is the stress tensor defined below. The properties of the spectra of Laplace operators as a function of geometry and type of the boundary is an old question going back to the 1911 work by Weyl [13]. For Neumann-type boundary conditions, which are

the case for a phonon billiard, the Weyl law establishes a *positive* mesoscopic correction to the density of states (DoS) proportional to the ratio of the perimeter, P , and area, A of the billiard [9, 14]. Specifically, for acoustic phonons in two dimensions, the correction to the total DoS is

$$\frac{1}{A} [N(\omega) - N_{\text{Bulk}}(\omega)] = \frac{\eta\omega}{4\pi c_{\perp}} \frac{P}{A} + o(\omega), \quad (1)$$

where $N(\omega) = \sum_{\omega_l \leq \omega} 1$ is the number of eigenvalues $\omega_l < \omega$, c_{\perp} (c_{\parallel}) is the velocity of transverse (longitudinal) phonons, and η is a positive dimensionless constant of order one, which for free-surface boundary conditions depends on the ratio c_{\perp}/c_{\parallel} only [14] (see appendix and Fig. 1). The longitudinal phonon DoS also acquires a positive correction (see, Fig. 1b), which eventually translates into an enhancement of the superconducting transition temperature.

$$\frac{T_c - T_{c0}}{T_{c0}} \propto \frac{\delta\lambda}{\lambda_{\text{bulk}}} \approx \frac{\eta_{\parallel} P}{2A k_D} \log \left(\frac{\omega_D}{\omega_0 e^{\chi}} \right) - \frac{\omega_0}{\omega_D}, \quad (2)$$

where $k_D = \omega_D/c_{\parallel} \sim a^{-1}$ is the Debye cutoff of order inverse lattice constant, whose exact value is determined by the total number of available phonon modes held constant for a given area, A . In Eq. (2), we assumed that the Fermi wavelength is the smallest length-scale. λ_{bulk} and $\delta\lambda$ respectively denote the bulk BCS coupling strength and its modification in our geometry. $\eta_{\parallel} \sim 1$ is a dimensionless constant plotted in the inset of Fig. 1b and $\omega_0 \sim c_{\parallel} \pi / \sqrt{A}$ is a non-universal low-energy cut-off of order finite-size quantization energy and $\chi = \log \frac{c_{\parallel} c_{\perp}}{(c_{\parallel}^2 + c_{\perp}^2)} \frac{\eta}{\eta_{\parallel}}$.

We consider a specific randomly generated shape shown in Fig. 1a, which is clearly chaotic. All numerical results are derived for this particular realization of a 2D grain, but due to self-averaging of relevant Eliashberg

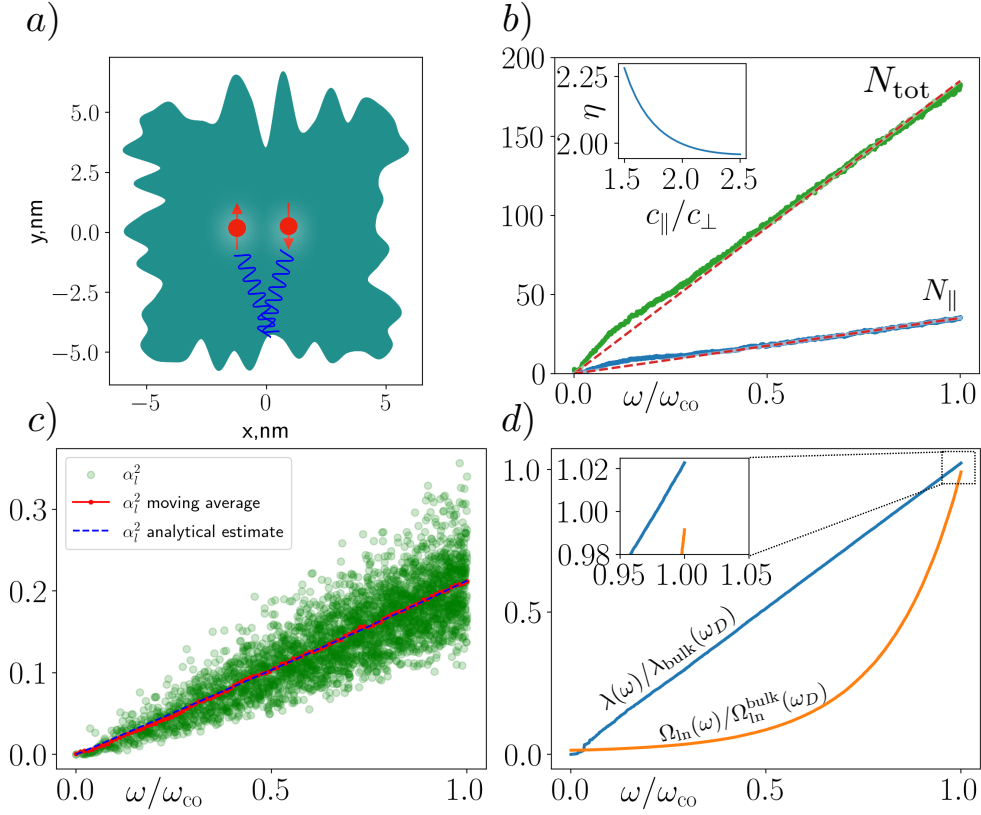


Figure 1. Electron pairing enhancement in chaotic grains. a) Schematic illustration of electron pairing in an irregular-shape metallic grain. b) The total and the longitudinal contributions to the phonon density of states, $\delta N(\omega) = N(\omega) - N_{\text{bulk}}(\omega)$, are shown in green and blue respectively. Red dashed lines are linear fits to the data including Eq. (1) for the total DoS. c) The Fermi surface averaging of the overlap of the phonon eigenfunctions, α_l , see Eq. ((9)), as a function of the eigenstate energy. d) Numerical results for the frequency-dependent BCS parameter $\lambda(\omega) \equiv 2 \int_0^\omega d\omega' \omega'^{-1} \alpha^2 F(\omega')$ and the logarithmic frequency cutoff $\Omega_{\text{ln}}(\omega) \equiv \omega_D \exp\left\{\frac{2}{\lambda} \int_0^\omega d\omega' \omega'^{-1} \ln(\omega'/\omega_D) \alpha^2 F(\omega')\right\}$. The superconducting transition temperature is determined by $\lambda = \lambda(\omega_{c0})$ and $\Omega_{\text{ln}} = \Omega_{\text{ln}}(\omega_{c0})$.

parameters, we are able to validate our specific computational data with generic analytical results rooted in random matrix theory. The starting point is the following electron-phonon Hamiltonian

$$H = \sum_{\sigma,m} \xi_m c_{m,\sigma}^\dagger c_{m,\sigma} + \sum_\ell \omega_\ell a_\ell^\dagger a_\ell + g \sum_\sigma \int_A d^2\mathbf{r} \nabla \cdot \vec{\Phi}(\mathbf{r}) \psi_\sigma^\dagger(\mathbf{r}) \psi_\sigma(\mathbf{r}), \quad (3)$$

where $\vec{\Phi}(\mathbf{r}) = \sum_\ell \frac{\vec{\phi}_\ell(\mathbf{r})}{\sqrt{2\omega_\ell}} (a_\ell + a_\ell^\dagger)$ and $\psi_{\sigma=\uparrow,\downarrow}(\mathbf{r}) = \sum_m \zeta_m(\mathbf{r}) c_{m,\sigma}$ are the phonon and electron operators respectively and g is the electron-phonon coupling. ξ_m and $\zeta_m(\mathbf{r})$ are the electron energies and wave-functions – the spectrum of the Schrödinger operator. Note that in real materials, the mean free path for electrons is often much smaller than the system size, $l \ll \sqrt{A}$ and hence random matrix theory description for electrons arises irrespective of boundary conditions. In contrast, ω_ℓ and $\vec{\phi}_\ell(\mathbf{r})$ are the phonon eigenfrequencies and eigenfunctions, which

are sensitive to the boundary and follow from the Navier-Cauchy equation [9] below

$$\rho \vec{\phi}_l \equiv -\rho \omega_\ell^2 \vec{\phi}_l = (\xi + \nu) \nabla \left(\nabla \cdot \vec{\phi}_l \right) + \nu \Delta \vec{\phi}_l, \quad (4)$$

where ξ and ν are Lamé parameters, ρ is the material density, and the two sound velocities are $c_{\parallel} = \sqrt{(\xi + 2\nu)/\rho}$, $c_{\perp} = \sqrt{\nu/\rho}$. We assume $c_{\parallel}/c_{\perp} = 2$ [15–17] and free-surface boundary condition. For a given grain geometry, Eq. (4) is solved using the finite-element methods available in open-source software [18]. The total bulk number of states below a certain energy ω is $N_{\text{Bulk}}(\omega) = \omega^2(c_{\parallel}^{-2} + c_{\perp}^{-2})/4\pi$.

We now generalize the Eliashberg theory of phonon-mediated Cooper pairing to chaotic grains. Define electronic Nambu spinor fields $\Psi(\mathbf{r}) = \{\psi_{\uparrow}(\mathbf{r}), \psi_{\downarrow}^{\dagger}(\mathbf{r})\}$ and the corresponding imaginary-time Green's function $\hat{\mathcal{G}}_{\mathbf{r},\mathbf{r}'}(\tau) = -\langle T \Psi(\mathbf{r},\tau) \otimes \Psi^{\dagger}(\mathbf{r}',0) \rangle$, where T is the time-ordering operator. The Nambu matrix-valued self-energy is given by: $\hat{\Sigma}_{\mathbf{r},\mathbf{r}'}(\tau) = -g^2 \mathcal{D}_{\mathbf{r},\mathbf{r}'}(\tau) \hat{\tau}_3 \hat{\mathcal{G}}_{\mathbf{r},\mathbf{r}'}(\tau) \hat{\tau}_3$ where $\hat{\tau}_i$ are Pauli matrices in Nambu space and

$\mathcal{D}_{\mathbf{r},\mathbf{r}'}(\tau) = -\left\langle T \left\{ \nabla \cdot \vec{\Phi}(\mathbf{r}, \tau) \nabla \cdot \vec{\Phi}(\mathbf{r}', 0) \right\} \right\rangle$. Furthermore, we include electronic disorder by means of an additional self-energy term $\hat{\Sigma}_{\mathbf{r}} = (4\pi\nu_0^F \tau_{\text{el}})^{-1} \hat{\tau}_3 \hat{\mathcal{G}}_{\mathbf{r},\mathbf{r}}(\tau) \hat{\tau}_3$, where ν_0^F is the electronic DoS at the Fermi energy and τ_{el} is the elastic scattering time. As we show in the SM in diffusive limit, the superconducting gap obeys the following local self-consistency equation:

$$\Delta(i\epsilon_n) = -g^2 \nu_0^F T \pi \sum_{n'} \mathcal{D}_{\text{eff}}(i\epsilon_n - i\epsilon_{n'}) \frac{\Delta(i\epsilon_{n'})}{|\epsilon_n| Z(i\epsilon_{n'})}, \quad (5)$$

where T is the temperature, $\epsilon_n = (2n+1)\pi T$ and Z is the quasiparticle renormalization factor. The effective phonon propagator is defined by:

$$\mathcal{D}_{\text{eff}}(i\Omega_n) = A^{-1} \int d^2\mathbf{r} d^2\mathbf{r}' J_0^2(k_F |\mathbf{r} - \mathbf{r}'|) \mathcal{D}_{\mathbf{r},\mathbf{r}'}(i\Omega_n), \quad (6)$$

where J_0 is the Bessel's function of the first kind, k_F is Fermi momentum and $\Omega_n = 2\pi n T$. Eqs. (5, 6) constitute the standard frequency-space Eliashberg equations [19] and we can thus estimate the critical temperature using McMillan-Allen-Dynes formula [20, 21]:

$$T_c = \frac{\Omega_{\text{ln}}}{1.2} \exp \left\{ -\frac{1.04(\lambda+1)}{\lambda - \mu^*(1+0.62\lambda)} \right\}. \quad (7)$$

Here, the effective BCS coupling strength and the logarithmic cut-off frequency are defined as $\lambda = 2 \int d\omega \omega^{-1} \alpha^2 F(\omega)$, $\Omega_{\text{ln}} = \omega_{\text{D}} \exp \left\{ \frac{2}{\lambda} \int d\omega \omega^{-1} \ln(\omega/\omega_{\text{D}}) \alpha^2 F(\omega) \right\}$, where ω_{D} is Debye energy, μ^* denotes Coulomb pseudo-potential which we set to 0.1 throughout and $\alpha^2 F(\omega)$ is the Eliashberg function [19, 22]:

$$\alpha^2 F(\omega) = \frac{g^2 \nu_0^F}{2A\omega} \sum_l \delta(\omega - \omega_l) \alpha_l^2 \quad (8)$$

where ν_{tot}^F is the electron density of states and the dimensionless matrix element of phonon eigenstates averaged of Fermi surface is

$$\alpha_l^2 = \int d^2\mathbf{r} d^2\mathbf{r}' C_l(\mathbf{r}) C_l(\mathbf{r}') J_0^2(k_F |\mathbf{r} - \mathbf{r}'|), \quad (9)$$

where ν_0^F is the electronic DoS at the Fermi energy and we defined the divergence as $C_l(\mathbf{r}) \equiv \nabla \cdot \vec{\phi}_l(\mathbf{r})$.

We now provide a numerical estimation of the critical temperature in the chaotic grain shown in Fig. 1 (a). Throughout this work we consider the limit $\xi \gg L \sim \sqrt{A}$, $k_F L \gg 1$, $L \gg l$, where l is the mean-free path and ξ is the superconducting coherence length in diffusive limit (see SM). Assuming the following parameters for Aluminum films $T_c^{\text{bulk}} = 1.2K$ [1] and $\omega_{\text{D}}/k_{\text{B}} \approx 428K$ we get the bulk parameters $\Omega_{\text{ln}}^{\text{bulk}}/\omega_{\text{D}} \approx 0.37$ and $\lambda_{\text{bulk}} \approx 0.44$. We note that within our model, we do not need the explicit knowledge of microscopic parameters such as g . For

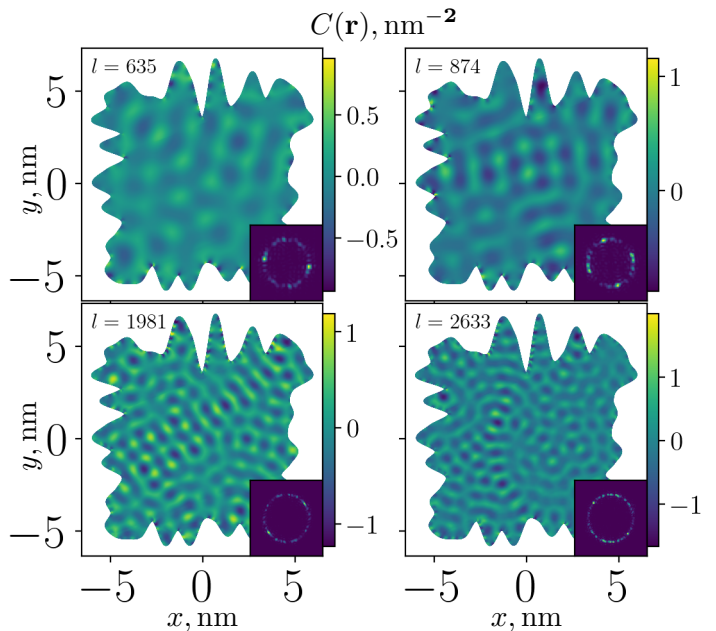


Figure 2. Divergencies of eigenvectors of Navier-Cauchy equations in chaotic grain. Insets show their Fourier transforms $|C(\mathbf{k})|^2$ for $k_x, k_y \in [-1.6k_l, 1.6k_l]$, where $k_l = \omega_l/c_{\parallel}$. Fourier transform is defined as $C(\mathbf{k}) = \int d^2\mathbf{r} C(\mathbf{r}) e^{-i\mathbf{k}\mathbf{r}}$.

the chaotic grain in Fig. 1 (a), the proper cutoff frequency $\omega_{\text{co}}/\omega_{\text{D}} \approx 0.97$ for $c_{\perp} = 3000\text{m/s}$. We now evaluate the matrix elements in Eq. (9) numerically (see Fig. (1) (c)) and find the modified BCS parameters $\lambda/\lambda_{\text{bulk}} \approx 1.023$ and $\Omega_{\text{ln}}/\Omega_{\text{ln}}^{\text{bulk}} \approx 0.99$. Combining these factors, we get the critical temperature enhancement $T_c/T_c^{\text{bulk}} \approx 1.1$.

To get further insight, we apply random matrix theory to phonon eigenvectors. Typical divergences of eigenvectors $C_l(\mathbf{r})$ and their Fourier transforms at high energies are shown in Fig. (2). In momentum space, we observe a random-speckle structure at momenta corresponding to the energy of the state. Relying on the arguments pioneered by Berry [9, 23, 24], we conjecture that at sufficiently short distances and sufficiently far away from the boundary, the correlation function of the phonon modes at high energies takes the following form (see also SM):

$$\overline{C_l(\mathbf{r}) C_l(\mathbf{r}')} \approx A^{-1} \frac{\nu_{\parallel}^{\text{ph}}(\omega_l) \omega_l^2}{\nu_{\text{tot}}^{\text{ph}}(\omega_l) c_{\parallel}^2} J_0 \left(\frac{\omega_l}{c_{\parallel}} |\mathbf{r} - \mathbf{r}'| \right), \quad (10)$$

where $\nu_{\parallel}^{\text{ph}}(\omega) = N_{\parallel}^{\text{ph}}(\omega)$ corresponds to the DoS of longitudinal phonons, which is $\nu_{\parallel}^{\text{ph}}(\omega) \equiv A^{-1} (\omega/c_{\parallel})^{-2} \int d^2\mathbf{r} \sum_l C_l(\mathbf{r}) C_l(\mathbf{r}) \delta(\omega - \omega_l)$. The resulting longitudinal DoS is shown in Fig. (2) (c), where we subtract the bulk contribution. We find that at high energies the DoS ν_{\parallel} follows Weyl's law $\delta\nu_{\parallel} \approx \eta_{\parallel} P / (4\pi A c_{\parallel})$ with $\eta_{\parallel} \approx 0.79$. With this scaling we can also benchmark our assumption in Eq. (10). In

Fig. (1) (c) we plot the matrix elements α^2 for different eigenstates and compare with the analytical formulas (10, 9) $\alpha^2(\omega) \approx \{\nu_{\parallel}^{\text{ph}}(\omega)/\nu_{\text{tot}}^{\text{ph}}(\omega)\}4\omega/\sqrt{4c_{\parallel}^2k_F^2 - \omega^2}$, where the total DoS $\nu_{\text{tot}}^{\text{ph}}(\omega) = N^{\text{ph}}(\omega)$. Together with Eqs. (8, 9) this yields the expression for the Eliashberg function at high energies:

$$\frac{\alpha^2 F(\omega)}{2g^2\nu_0^F} \approx \frac{\nu_{\parallel}^{\text{ph}}(\omega)}{\sqrt{4c_{\parallel}^2k_F^2 - \omega^2}}, \quad (11)$$

Eq. (11) implies log-singular corrections to the electron-phonon interaction parameter λ , since the density of states is non-vanishing at low energies according to Weyl's law Eq. (1). However, our treatment is valid only at sufficiently large energies and therefore we will have to impose a low-energy finite-size cut-off ω_0 which is sensitive to grain geometry and can be found by fitting to numerical data. By doing so, we find $\omega_0 \sim \pi c_{\parallel}/\sqrt{A}$ for longitudinal phonons.

We note that the enhancement of T_c is a direct consequence of the Weyl's law which implies softening of phonons associated with the slower scaling of the density of states. Combining Eq. (11), and taking into account the high- and low-energy cut-offs we get the analytical estimate for the T_c enhancement provided in Eq. (2) which, in our parameter regime, comes predominantly from the BCS coupling strength renormalization. We note that the low-energy cut-off is non-universal and can potentially be different for other grain geometries.

In conclusion we note the existence of an optimal size of a grain for a given shape. Fixing the dimensionless parameter, $\zeta = P/\sqrt{A}$, and varying T_c (2) over the characteristic size, \sqrt{A} , we find the optimal condition as follows

$$1 = \frac{\omega_0}{\omega_D} \exp\left(\frac{2A}{P\eta_{\parallel}} \frac{\omega_0}{c_{\parallel}} + \frac{c_{\perp}c_{\parallel}}{c_{\perp}^2 + c_{\parallel}^2} \frac{\eta}{\eta_{\parallel}} + \eta_{\parallel}\right)$$

The corresponding change in the BCS strength is given by: $\delta\lambda/\lambda_{\text{bulk}} \approx \frac{\eta_{\parallel}\zeta}{2\pi} \exp\left\{-\frac{2\pi}{\eta_{\parallel}\zeta} - \frac{c_{\perp}c_{\parallel}}{c_{\perp}^2 + c_{\parallel}^2} \frac{\eta}{\eta_{\parallel}} - 1\right\}$. We thus find that the critical temperature have a strong dependence on the grain geometry. For example for a circular grain $\zeta_0 = 2/\sqrt{\pi}$, while for our grain $\zeta \approx 6.4$, which is significantly larger. Clearly, the geometry can be further optimized to create grains with a higher T_c for a given material.

Real granular superconductors are composed of a variety of grains of different shapes and sizes. Each grain has its own T_c and there is a probability distribution of transition temperatures in the material. The overall positive shift – Eq. (2) – corresponds to the average transition temperature $\langle T_c \rangle$. However, even for $T > \langle T_c \rangle$, there will exist a subset of grains with higher individual transition

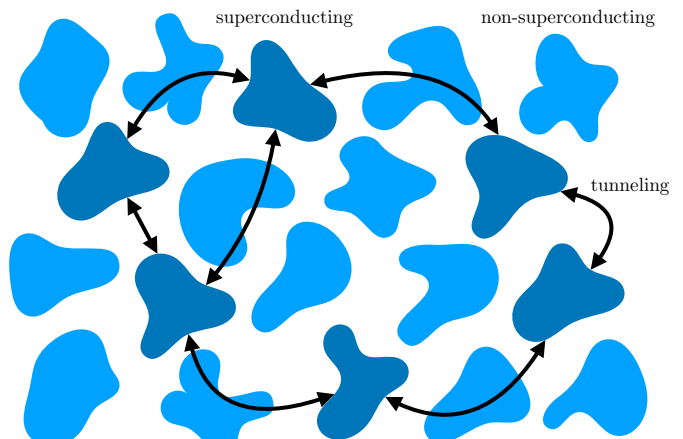


Figure 3. A schematic illustration of a superconducting Josephson network of superconducting grains with random geometries. Dark and light blue regions represent superconducting and non-superconducting grains respectively. Arrows represent Josephson tunneling between the grains.

temperature. The global superconducting critical point in such a system is determined by a percolation transition where a Josephson network of coupled superconducting grains spanning the entire sample first appears. This temperature can be considerably higher than $\langle T_c \rangle$, and such mesoscopic grain fluctuations provide another mechanism for enhancing superconductivity in granular materials similar to [25, 26].

The authors thank Andy Millis, Amit Vikram, and Masoud Mohammadi for useful discussions. This work was supported by U.S. Department of Energy, Office of Science, Basic Energy Sciences under Award No. DE-SC0001911 (analytical random matrix theory by V.G. and A.G.) and DARPA HR00112490310 (numerical simulations).

-
- [1] B. Abeles, R. W. Cohen, and G. Cullen, *Physical Review Letters* **17**, 632 (1966).
 - [2] A. Thomas, E. Devaux, K. Nagarajan, T. Chervy, M. Seidel, D. Hagenmüller, S. Schütz, J. Schachenmayer, C. Genet, G. Pupillo, *et al.*, arXiv preprint arXiv:1911.01459 (2019).
 - [3] V. N. Smolyaninova, C. Jensen, W. Zimmerman, J. C. Prestigiacomo, M. S. Osofsky, H. Kim, N. Bassim, Z. Xing, M. M. Qazilbash, and I. I. Smolyaninov, *Scientific reports* **6**, 34140 (2016).
 - [4] R. W. Cohen and B. Abeles, *Physical Review* **168**, 444 (1968).
 - [5] M. Strongin, O. Kammerer, J. Crow, R. Parks, D. Douglass Jr, and M. Jensen, *Physical Review Letters* **21**, 1320 (1968).
 - [6] S. Prischepa and V. Kushnir, *Journal of Physics: Condensed Matter* **35**, 313003 (2023).
 - [7] A. M. García-García, J. D. Urbina, E. A. Yuzbashyan,

- K. Richter, and B. L. Altshuler, *Physical Review B—Condensed Matter and Materials Physics* **83**, 014510 (2011).
- [8] A. M. García-García, J. D. Urbina, E. A. Yuzbashyan, K. Richter, and B. L. Altshuler, *Physical review letters* **100**, 187001 (2008).
- [9] G. Tanner and N. Søndergaard, *Journal of Physics A: Mathematical and Theoretical* **40**, R443 (2007).
- [10] A. O. E. Animalu, F. Bonsignori, and V. Bortolani, *Il Nuovo Cimento B (1965-1970)* **44**, 159 (1966).
- [11] J. Achenbach, A. Gautesen, and H. McMaken, *Ray Methods for Waves in Elastic Solids: with Applications to Scattering by Cracks* (Pitman Advanced Publishing Program, 1982).
- [12] L. D. Landau, L. Pitaevskii, A. M. Kosevich, and E. M. Lifshitz, *Theory of elasticity: volume 7*, Vol. 7 (Elsevier, 2012).
- [13] H. Weyl, *Nachrichten von der Gesellschaft der Wissenschaften zu Göttingen, Mathematisch-Physikalische Klasse* **1911**, 110 (1911).
- [14] P. Bertelsen, C. Ellegaard, and E. Hugues, *The European Physical Journal B-Condensed Matter and Complex Systems* **15**, 87 (2000).
- [15] S. Fassbender, B. Hoffmann, and W. Arnold, *Materials Science and Engineering: A* **122**, 37 (1989).
- [16] R. David, H. Van der Laan, and N. Poulis, *Physica* **29**, 357 (1963).
- [17] D. R. Lide, *CRC handbook of chemistry and physics*, Vol. 85 (CRC press, 2004).
- [18] I. A. Baratta, J. P. Dean, J. S. Dokken, M. Habera, J. S. Hale, C. N. Richardson, M. E. Rognes, M. W. Scroggs, N. Sime, and G. N. Wells, “DOLFINx: The next generation FEniCS problem solving environment,” (2023).
- [19] F. Marsiglio, *Annals of Physics* **417**, 168102 (2020).
- [20] W. McMillan, *Physical Review* **167**, 331 (1968).
- [21] P. B. Allen and R. Dynes, *Physical Review B* **12**, 905 (1975).
- [22] G. Ummarino *et al.*, *Emergent Phenomena in Correlated Matter* **3**, 13 (2013).
- [23] M. V. Berry, *Nonlinearity* **1**, 399 (1988).
- [24] A. Akolzin and R. L. Weaver, *Physical Review E—Statistical, Nonlinear, and Soft Matter Physics* **70**, 046212 (2004).
- [25] V. Galitski and A. Larkin, *Physical Review Letters* **87**, 087001 (2001).
- [26] V. Galitski, *Phys. Rev. B* **77**, 100502 (2008).
- [27] U. Kuhl, H. Stöckmann, and R. Weaver, *Journal of Physics A: Mathematical and General* **38**, 10433 (2005).
- [28] W. Belzig, C. Bruder, and G. Schön, *Physical Review B* **54**, 9443 (1996).
- [29] W. Belzig, F. K. Wilhelm, C. Bruder, G. Schön, and A. D. Zaikin, *Superlattices and microstructures* **25**, 1251 (1999).
- [30] F. S. Bergeret, A. F. Volkov, and K. B. Efetov, *Europhysics Letters* **66**, 111 (2004).

Appendix A: Navier-Cauchy equations

Here we review the elastic equations inside a grain. We define the local lattice displacement vector $\vec{\phi}$ obeying [9]:

$$\rho \frac{d^2}{dt^2} \vec{\phi} = \nabla \cdot \hat{\sigma}(\vec{\phi}),$$

where ρ is the material density and σ is the stress tensor,

$$\hat{\sigma}(\vec{\phi}) = \xi \mathbf{1} \text{Tr} \hat{\epsilon} + 2\nu \hat{\epsilon}$$

where λ and μ are Lamé constants and the strain tensor is assumed to be

$$\epsilon_{i,j} = \frac{1}{2} (\partial_j \phi_i + \partial_i \phi_j)$$

With this, we get:

$$\rho \frac{d^2}{dt^2} \phi_i = \sum_j \partial_j \sigma_{j,i}(\vec{\phi}) = (\xi + \nu) \partial_i \sum_j \partial_j \phi_j + \nu \sum_j \partial_j^2 \phi_i,$$

or in the vector form:

$$\rho \frac{d^2}{dt^2} \vec{\phi} = (\xi + \nu) \nabla (\nabla \cdot \vec{\phi}) + \nu \Delta \vec{\phi},$$

The coefficients λ and μ can be straightforwardly related to bulk sound velocities. Indeed, in Fourier space we get:

$$\omega^2 \vec{\phi}_{\mathbf{k}} = \frac{\xi + \nu}{\rho} \mathbf{k} (\mathbf{k} \cdot \vec{\phi}_{\mathbf{k}}) + \frac{\nu}{\rho} k^2 \vec{\phi}_{\mathbf{k}}$$

Projecting onto the longitudinal and transverse components we get: $\omega = \sqrt{\frac{\xi + 2\nu}{\rho}} k$ and $\omega = \sqrt{\nu/\rho} k$. The longitudinal speed of sound is thus $c_{\parallel} = \sqrt{\frac{\xi + 2\nu}{\rho}}$.

In our calculations, we assume the free-surface boundary conditions, which are equivalent to the absence of restoring force at the boundary $\mathbf{n} \cdot \hat{\sigma}(\vec{\phi}) = 0$, where \mathbf{n} is the normal vector to the boundary.

Appendix B: Derivation of the eigenvector ansatz

Here we provide a heuristic derivation of the eigenvector ansatz Eq. (10) following conventional argument related to the short-distance correlations in chaotic systems. More precisely, we define: $f_A(\omega, \mathbf{r}, \mathbf{r}') = \sum_l C_l(\mathbf{r}) C_l(\mathbf{r}') \delta(\omega - \omega_l)$, where $C_l(\mathbf{r})$ is the eigenvector divergence. The correlation function of divergences can now be inferred from f assuming an unbounded system as follows [14, 23, 27]:

$$\overline{C_l(\mathbf{r}) C_l(\mathbf{r}')} = A^{-1} \nu_{\text{tot}}^{-1}(\omega) f_{\infty}(\omega |\mathbf{r} - \mathbf{r}'|),$$

where $f_\infty = \lim_{A \rightarrow \infty} f_A$.

$$\begin{aligned} f_\infty(\omega, \mathbf{r}, \mathbf{r}') &= \int \frac{d^2 \mathbf{k}}{(2\pi)^2} k^2 e^{i\mathbf{k}\mathbf{r}} \delta(\omega - c_\parallel k) \\ &= \nu_\parallel(\omega) \frac{\omega^2}{c_\parallel^2} J_0\left(\frac{\omega}{c} |\mathbf{r} - \mathbf{r}'|\right) \end{aligned}$$

where J_0 is Bessel's function of the first kind and $\nu_\parallel(\omega)$ is the longitudinal density of states.

Appendix C: Weyl's law for phonon billiards with free-surface boundary conditions

Here we provide an explicit expression for the Weyl parameter, η , used in Eq. (1). This parameter was derived in Ref. [14] as follows

$$\begin{aligned} \eta &= \frac{4}{\sqrt{\gamma}} - 3 + \frac{1}{\kappa} \\ &+ \frac{4}{\pi} \int_{1/\kappa}^1 \arctan \left\{ \frac{(t^2 - 1)^2}{4t^2 \sqrt{1 - t^2} \sqrt{t^2 - \frac{1}{\kappa^2}}} \right\} dt, \end{aligned} \quad (\text{C1})$$

where $\kappa = c_\parallel/c_\perp$ and γ is a solution to the following equation belonging to the interval]0, 1[:

$$\gamma^3 - 8\gamma^2 + 8 \left(3 - \frac{2}{\kappa^2}\right) \gamma - 16 \left(1 - \frac{1}{\kappa^2}\right) = 0 \quad (\text{C2})$$

We note that the value of η is agreement with our numerical simulations.

Appendix D: Diffusive limit

Here we derive the effective interaction within the quasi-classical approximation [28–30] assuming the interaction is changing sufficiently slowly in space which is the case in our parameter regime $k_D < k_F$. We start by rewriting the self-energy equation in momentum space for the relative coordinate:

$$\begin{aligned} \hat{\Sigma}_{\mathbf{R}, \mathbf{k}}(i\epsilon_n) &= \\ &- \frac{1}{\beta A} \sum_{n'} \sum_{\mathbf{k}'} \mathcal{D}_{\mathbf{R}, \mathbf{k}-\mathbf{k}'}(i\epsilon_n - i\epsilon_{n'}) \hat{\tau}_3 \hat{G}_{\mathbf{R}, \mathbf{k}'}(i\epsilon_{n'}) \hat{\tau}_3, \end{aligned}$$

where we performed the Fourier transform with respect to the relative coordinate. The center-of-mass (COM) coordinate is defined as $\mathbf{R} = (\mathbf{r} + \mathbf{r}')/2$. In the following, we perform a quasi-local approximation for the phonon propagator by restricting both momenta to the Fermi surface [20, 21]. In this case, the self-energy depends only on the COM coordinate. Disorder scattering can be

added in a similar way as we discuss in the main text. We now consider a quasiclassical approximation for electrons by defining $\hat{g}_{\mathbf{R}} \equiv \frac{i}{\pi} \int d\xi_k \hat{\tau}_3 \hat{G}_{\mathbf{R}, \mathbf{k}}$, which obeys the Usadel equation in the diffusive limit:

$$D \nabla (\hat{g}_{\mathbf{R}} \nabla \hat{g}_{\mathbf{R}}) = - \left[\hat{g}_{\mathbf{R}}, \epsilon_n \tau_3 + i \hat{\Sigma}_{\mathbf{R}} \tau_3 \right], \quad (\text{D1})$$

where $D = v_F^2 \tau_{\text{el}}/2$ is the diffusion coefficient, τ_{el} denotes the disorder scattering rate and we restricted the self-energy to its value on the Fermi surface $\hat{\Sigma}_{\mathbf{R}}(i\epsilon_n) \equiv \hat{\Sigma}_{\mathbf{R}, k=k_F}(i\epsilon_n)$ according to the local approximation. The vacuum boundary condition for the quasiclassical Green's function is given by $\mathbf{n} \cdot \nabla \mathbf{g}_{\mathbf{R}} = \mathbf{0}$, where \mathbf{n} is the vector normal to the boundary. We also perform the standard quasi-local approximation for the self-energy:

$$\hat{\Sigma}_{\mathbf{R}}(i\epsilon_n) = \frac{1}{\beta} \nu_0^F i\pi \sum_{n'} \langle \mathcal{D}_{\mathbf{R}, \mathbf{k}_F - \mathbf{k}'_F}(i\epsilon_n - i\epsilon_{n'}) \rangle \hat{g}_{\mathbf{R}}(i\epsilon_{n'}) \hat{\tau}_3,$$

where the phonon propagator is averaged over direction of the difference of two Fermi wavevectors $\mathbf{k}_F - \mathbf{k}'_F$ and ν_0^F is the fermion density of states. We now look for a critical temperature and linearize the Usadel's equation with respect to the anomalous component. To this end we use the ansatz $g_{\mathbf{R}} = g^{(0)} + f_{\mathbf{R}} = \text{sign} \epsilon_n \tau_3 + f_{\mathbf{R}}$, where $f_{\mathbf{R}}$ is purely off-diagonal. We write the local self-energy in the conventional form $i \hat{\Sigma}_{\mathbf{R}} \tau_3 \approx Z_{\mathbf{R}}(i\epsilon_n) \tau_0 + \Delta_{\mathbf{R}}(i\epsilon_n) \tau_1$, where Z is the quasiparticle renormalization factor and $\Delta_{\mathbf{R}}$ is the gap. From Eq. (D1) we get:

$$D \nabla^2 \hat{f}_{\mathbf{R}} = -2\tau_1 \Delta_{\mathbf{R}} + 2|\epsilon_n| Z_{\mathbf{R}}(i\epsilon_n) \hat{f}_{\mathbf{R}}, \quad (\text{D2})$$

The characteristic length of this diffusion equation is thus given by the coherence length of the superconductor $\xi \approx \sqrt{D/(2\pi T \overline{Z}_{\mathbf{R}})}$ as expected. In the limit when the coherence length is large, the $f_{\mathbf{R}}$ changes little between the boundaries and we can write

$$\hat{f}_{\mathbf{R}} \approx \frac{\tau_1 \overline{\Delta_{\mathbf{R}}}(i\epsilon_n)}{|\epsilon_n| \overline{Z_{\mathbf{R}}}(i\epsilon_n)}$$

where the averaging is taken over the grain area. The self-consistency equation becomes:

$$\Delta_{\mathbf{R}}(i\epsilon_n) = -\frac{1}{\beta} \nu_0 \pi \sum_{n'} \langle \mathcal{D}_{\mathbf{R}, \mathbf{k}_F - \mathbf{k}'_F}(i\epsilon_n - i\epsilon_{n'}) \rangle \frac{\overline{\Delta_{\mathbf{R}}}(i\epsilon_{n'})}{|\epsilon_n| \overline{Z_{\mathbf{R}}}(i\epsilon_{n'})}.$$

We note that $\Delta_{\mathbf{R}}$ is simply the self-energy and it is not equivalent to the superconducting gap which is uniform. Moreover, we are interested in averaging over the grain area (since it defines T_c and the actual gap):

$$\overline{\Delta_{\mathbf{R}}}(i\epsilon_n) = -\frac{1}{\beta} \nu_0 \pi \sum_{n'} \overline{\langle \mathcal{D}_{\mathbf{R}, \mathbf{k}_F - \mathbf{k}'_F}(i\epsilon_n - i\epsilon_{n'}) \rangle} \frac{\overline{\Delta_{\mathbf{R}}}(i\epsilon_{n'})}{|\epsilon_n| \overline{Z_{\mathbf{R}}}(i\epsilon_{n'})}.$$

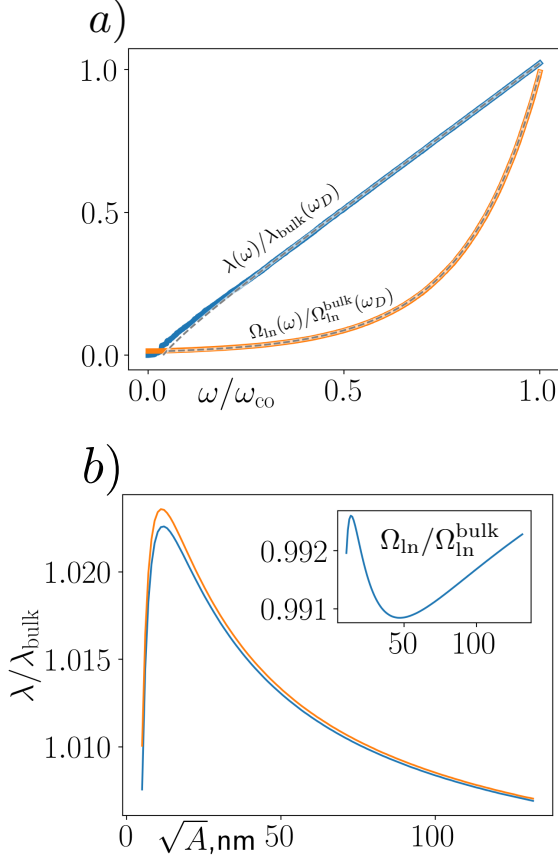


Figure 4. Fit of the numerical data for $\lambda(\omega)$ and $\Omega_{ln}(\omega)$. Grey dashed lines are fits using Eq. (11) with $\omega_0 \approx 1.1c_{\parallel}/\sqrt{A}$ for the BCS pairing strength and $\omega_0 \approx 1.5c_{\parallel}/\sqrt{A}$ for the logarithmic cut-off frequency.

Let us now explicitly derive the interaction (note that integral can be taken over the infinite space):

$$\begin{aligned} \overline{\langle \mathcal{D}_{\mathbf{R}, \mathbf{k}_F - \mathbf{k}'_F}(i\Omega_n) \rangle} &\equiv \int \frac{d^2 \mathbf{R}}{A} \mathcal{D}_{\mathbf{R}, \mathbf{k}_F - \mathbf{k}'_F}(i\Omega_n) = \\ &= \int \frac{d^2 \mathbf{R}}{A} \int d^2 \mathbf{r} \langle e^{-i(\mathbf{k}_F - \mathbf{k}'_F) \cdot \mathbf{r}} \rangle \mathcal{D}_{\mathbf{R}, \mathbf{r}}(i\Omega_n) \\ &= A^{-1} \int d^2 \mathbf{r} d^2 \mathbf{r}' J_0^2(k_F |\mathbf{r} - \mathbf{r}'|) \mathcal{D}_{\mathbf{r}, \mathbf{r}'}(i\Omega_n) \end{aligned}$$

Which is the same interaction as in the main text.

We now provide details of an analytical estimation of the transition temperature in Eq. (2). We first compute the BCS pairing strength and the logarithmic cut-off frequency exactly numerically and with the approximate Eliashberg function Eq. (11) as shown in Fig. (4) (a). The non-universal low-energy behavior is modeled as a sharp cut-off. We find a nearly perfect fits with our analytical estimate of spectral density Eq. (11).

Let us now assume that we fix the grain shape but perform a scaling transformation. We assume the low-energy cut-off frequencies are scaled accordingly. At the same time, the high-energy behavior is correctly captured by our analytical expression Eq. (11). Within these assumptions we find in the analytically tractable limit $k_F \rightarrow \infty$ and expanding in the system size $P/A \sim L^{-1}$, $\omega_0 \sim L^{-1}$:

$$\frac{\lambda - \lambda_{\text{bulk}}}{\lambda_{\text{bulk}}} \approx \frac{\eta_{\parallel} P}{2A k_D} \left\{ \log \left(\frac{\omega_D}{\omega_0 e^{\chi}} \right) \right\} - \frac{\omega_0}{\omega_D}$$

In Fig. (4) (b) we compare this approximation with the exact integral over Eliashberg function Eq. (11). We find a reasonably good agreement. We also numerically estimate the change in Ω_{ln} which is found to be small and we assume it can be absorbed into the frequency cut-off of the BCS constant.

1. Critical temperature

We now discuss how the change in the BCS strength λ and the cut-off frequency Ω_{ln} affect the critical temperature. From Eq. (7) we get

$$\frac{\delta T_c}{T_c} \approx 4.74 \frac{\lambda - \lambda_{\text{bulk}}}{\lambda_{\text{bulk}}},$$

where we used our estimation of the bulk pairing strength $\lambda_{\text{bulk}} \approx 0.44$.